PHYSICAL REVIEW B **83**, 161403(R) (2011)

Observation of intrinsic intraband π-plasmon excitation of a single-layer graphene

S. Y. Shin,[1] C. G. Hwang,[2] S. J. Sung,[1] N. D. Kim,[3] H. S. Kim,[1] and J. W. Chung[1,*]
[1]*Department of Physics, Pohang University of Science and Technology, Pohang 790-784, Korea*
[2]*Materials Sciences Division, Lawrence Berkeley National Laboratory, Berkeley, California 94720 USA*
[3]*Department of Chemistry, Pohang University of Science and Technology, Pohang 790-784, Korea*
(Received 11 January 2011; published 18 April 2011)

We report the energy-momentum dispersion $\omega(q)$ of a low-energy intraband π plasmon arising from Dirac fermions in the conduction band of a single-layer graphene (SLG), not complicated by couplings with other excitations. For a wide range of q ($0.39 \leqslant q/k_F \leqslant 2.36$), where $k_F = 0.061$ Å^{-1} is the Fermi wave vector, the intraband plasmon survives through the interband single-particle excitation (SPE) region, and linearly disperses beyond the Landau damping $q_c = 0.90\ k_F$ asymptotically approaching the boundary of the interband SPE without ever entering the intraband SPE. Such a unique feature is completely distinct from the plasmon of either a multilayer graphene or a normal two-dimensional electron gas, and hence demonstrates another intrinsic nature of Dirac fermions in SLG.

DOI: 10.1103/PhysRevB.83.161403 PACS number(s): 68.65.Pq, 73.20.Mf, 73.22.−f, 73.22.Pr

A single-layer graphene (SLG) has many unique and exotic properties that have no counterpart in conventional two-dimensional (2D) electrons systems.[1] The characteristic conical Dirac bands of SLG near the K point of the hexagonal brillouin zone[1,2] cause such peculiar features, for example, the anomalous quantum Hall effect (QHE).[1] The intrinsic nature of SLG, however, is found to vary sensitively with a disturbing environment through additional interactions of Dirac fermions with other low-energy excitations. Added adsorbates on SLG often modify the conical bands near the Dirac point,[3,4] and the anomalous half-integer QHE of SLG returns back to a normal integer QHE on the bilayer graphene.[1] Similarly, the characteristic Raman peaks, G and 2D, of graphene shift in a delicate fashion with an increasing number of graphene layers.[5,6] Here, we report another intrinsic nature of SLG, the energy-momentum dispersion $\omega(q)$ of intraband π plasmon, which is a collective excitation of Dirac electrons in the conduction band. We also show its subtle evolution upon increasing the number of graphene layers. As predicted earlier by theory,[7,8] our measured $\omega(q)$ using high-resolution electron-energy-loss spectroscopy (HREELS) reveals a totally different behavior from that of a typical 2D electrons system. The dispersion changes sensitively with the presence of small fractions of few-layer graphene (FLG). The characteristic linear Dirac bands of SLG thus not only bring forth the linear behavior of the interband π plasmon observed above 4.5 eV in SLG[9] or in the individualized single-wall carbon nanotubes,[10] but also the intrinsic $\omega(q)$ of the intraband π plasmon from SLG, far different from a parabolic dispersion of FLG or graphite.[9,10]

Although the dynamical dielectric function $\varepsilon(q,\omega)$ of a doped graphene calculated within the random phase approximation (RPA) has been predicted to be quite different from the one in normal 2D electrons systems,[7,8] most earlier HREELS data from SLG,[11–14] however, have been described in terms of the Stern's RPA formula derived for a normal 2D electrons system.[15] Since the formation of a large-scale SLG comparable to the size of the incoming probe, typically about 1 mm in diameter, has not yet been available, most SLG samples are likely to contain randomly distributed micron-sized SLG domains. Moreover a minor fraction of multilayer graphenes inevitably coexisting with SLG often complicates the interpretation of such data intended for SLG. Additional mechanisms, therefore, have been invoked to explain any deviation from the Stern's RPA formula.[12–14] We show that the intraband π plasmon measured from a SLG-abundant sample, not complicated by the multilayer effects, is best described by the theoretical $\varepsilon(q,\omega)$ devised solely for a doped SLG.

We prepared a SLG-abundant sample by removing silicon atoms from an *n*-type 6H-SiC(0001) surface through annealing under UHV as well documented earlier to form a good quality SLG.[16,17] The formation of SLG was monitored by a combination of several probing tools including a high spatial resolution low-energy electron diffraction (LEED),[18] angle-resolved photoemission spectroscopy (ARPES),[2,4,17,19] and HREELS with a Leybold-Heraeus ELS-22 spectrometer. In order to avoid the sample complicated by a small fraction of graphene multilayers, we have intentionally selected an initial stage of forming SLG onto the insulating $6\sqrt{3} \times 6\sqrt{3}$-R30° ($6\sqrt{3}$ for short) buffer layer. We confirmed this early stage of SLG by deliberately monitoring the change in Fuchs-Kliewer (F-K) phonon energy, which sensitively changes during the graphitization process. The optimum energy resolution and the half-acceptance angle of the HREELS detector were 19 meV and 2°, respectively. The annealing temperature T_a was measured by an optical pyrometer.[20] The well-characterized evolution of the LEED pattern upon forming graphene layers on the 6H-SiC(0001) surface begins with a Si-rich 3×3 phase formed at $T_a = 830$ °C under Si flux, which develops into the $\sqrt{3} \times \sqrt{3}$-R30° ($\sqrt{3}$ for short) phase when annealed at $T_a = 980$°C. Upon annealing further at $T_a = 1150$ °C, the carbon-rich insulating $6\sqrt{3}$ buffer layer appears. SLG begins to form on the buffer layer when annealed at slightly higher temperature with the LEED pattern maintaining nearly the same symmetry.[18] Although there is a subtle but discernible change in the LEED pattern indicating the formation of SLG, we find the most convincing evidence from the change in HREELS spectra as shown in Fig. 1. Note that each intermediate phase during the graphitization process in Fig. 1(a) has its own characteristic loss peak.

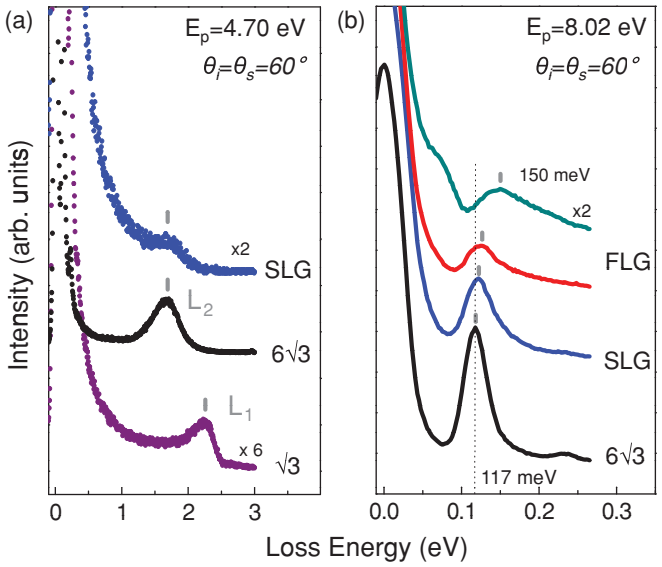

FIG. 1. (Color online) (a) HREELS spectra revealing its characteristic loss peak for the $\sqrt{3}$ phase, the $6\sqrt{3}$ phase, and SLG obtained with the energy of probing electrons $E_p = 4.70$ eV at a specular geometry. (b) Spectral change of F-K phonon peak identifying each intermediate phase with its characteristic loss energy; at 117 meV for the $6\sqrt{3}$ phase, 120 ± 1.0 meV for SLG, gradually increasing up to 150 meV for FLG. $E_p = 8.02$ eV.

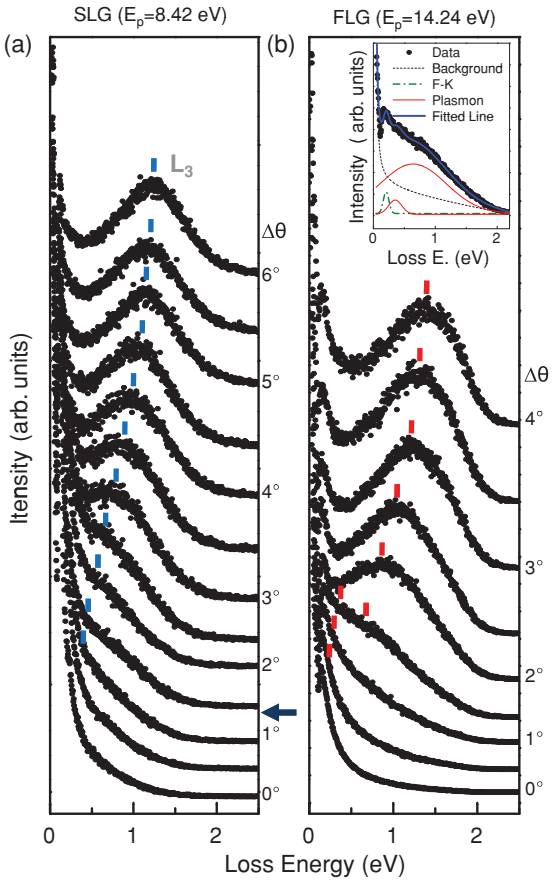

FIG. 2. (Color online) Variation of L_3 loss peak with increasing scattering angle (θ) measured from (a) SLG and (b) FLG. The angle $\Delta\theta$ represents the off-angle from the specular geometry and the arrow indicates q_c of Landau damping. All spectra are vertically shifted and magnified to make L_3 visible. One notes that L_3 shifts toward the higher loss energy side and becomes split into two peaks in FLG. Inset shows the details of subpeaks used in the fitting ($\Delta\theta = 1.5°$).

The L_1 loss peak at about 2.30 eV from the $\sqrt{3}$ phase disappears when the $6\sqrt{3}$ phase is formed with its unique loss peak L_2 at 1.70 eV. As SLG begins to form on the buffer layer, the L_2 loses its spectral weight and eventually almost disappears when SLG is covered most of the underlying surface area. The much-enhanced Drude tail from the metallic SLG is another signature for SLG. The L_1 peak indicates an inter-Hubbard band transition.[21] Since the buffer layer with the linear Dirac bands not yet formed has four major flat surface bands, at 0.5 and 1.6 eV below Fermi level,[19] and at 1.0 and 2.4 eV above Fermi level, respectively,[22] the L_2 can be safely ascribed to an interband transition from -0.5 to 1.0 eV.

Although SLG can be readily identified by the spectral features described above, the early stage of forming SLG not complicated by any coexisting FLG demands further experimental evidence. Figure 1(b) shows the change of F-K phonon energy $\hbar\omega_{FK}$ during the graphitization process as also seen for Raman peaks G and 2D.[5,6] The loss energy $\hbar\omega_{FK} =$ 117 meV (bottom curve) well identified as the F-K phonon from the buffer layer[9] upshifts to $\hbar\omega_{FK} = 120 \pm 1.0$ meV showing an asymmetric line shape due to the nearby weak loss peak from SLG. As SLG develops further, the F-K peak weakens quickly while broadening at the same time until its energy reaches up to $\hbar\omega_{FK} = 150$ meV when FLG is developed.[11,12,23] The early stage of SLG, therefore, can be determined unambiguously and *in situ* by carefully monitoring the change in energy of the F-K loss peak.

We show the change of its characteristic loss peak L_3 of SLG thus prepared with increasing the scattering angle $\Delta\theta$ in Fig. 2(a). We identify L_3 as a low-energy intraband π plasmon of SLG,[11] which is distinct from the interband plasmon observed above 4.5 eV. The energy range and broad linewidth of L_3 simply exclude the possibility of a local vibrational origin. Furthermore, it may not be an interband electronic transition since the dispersion extends down to a small momentum region, far below q_c in Fig. 3, where no relevant electronic states are available. It is also different from the loss peak arising from FLG as shown in Fig. 2(b), which exhibits quite a different dispersion.

We now confirm that the SLG of $\hbar\omega_{FK} = 120$ meV shown in Fig. 2(a) represents the early stage formed on the insulating buffer layer so that the SLG is neither electrically mixed with its substrate nor complicated by any significant portion of FLG, if any. The dispersion $\omega(q)$ extracted from Fig. 2(a) should, therefore, represent another intrinsic feature of a pure SLG, that is, to be compared with theory derived for SLG. As shown in inset of Fig. 2(b), we have fitted the spectra in Fig. 2(a) with two Gaussian functions representing the contributions from the F-K phonon and plasmon after subtracting the background.[24] The data from the fits are presented in Fig. 3. Notice that we have no complication in the distribution of the data points indicating the coupling with F-K phonons,[12] defects,[13] or any resonance effect of electron-hole pairs[14] as reported earlier based on the Stern's formula. We have thus compared our

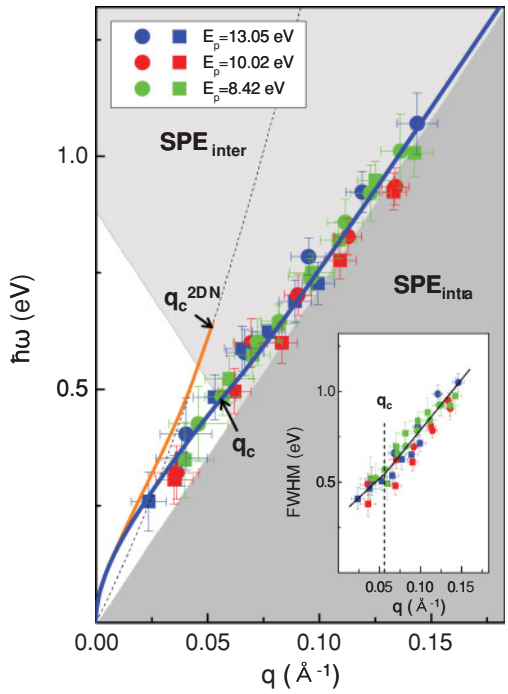

FIG. 3. (Color online) The calculated dispersion (blue solid curve) of the intraband π-plasmon best describing the measured data (filled symbols) obtained from SLG. Grey regions show the two single-particle excitations (SPE) by intra (right) and interband (left) electron-hole pair productions. Inset shows that the plasmon continues to broaden its line-width with increasing q, surviving even after q_c (Landau damping). The light red curve and the dotted curve represent a calculated plasmon dispersion and SPE of 2D normal electrons (2DN).

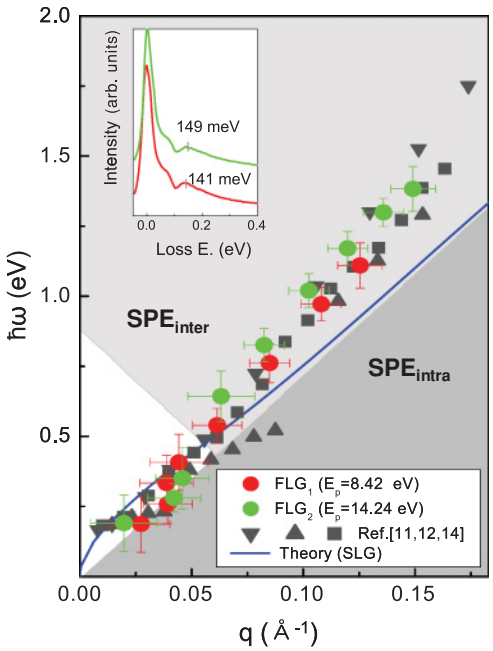

FIG. 4. (Color online) The measured data (colored circles) showing the dispersions of plasmon excitations from FLG. Our data obtained from two different layers of graphene agree with those in previous work (black symbols). Inset shows the two FK phonons to identify different layers of graphene.

data with theory developed for SLG.[7,8] The collective plasmon mode within RPA is given by the zeros of dynamical dielectric function,

$$\varepsilon(q,\omega) = 1 + v(q)\Pi(q,\omega) = 0, \qquad (1)$$

where $v(q) = 2\pi e^2/\kappa q$ is the 2D Coulomb interaction in the q space. The 2D polarizability $\Pi(q,\omega)$ includes contributions from both conduction band $\Pi^+(q,\omega)$ and valence band $\Pi^-(q,\omega)$ for a doped graphene with the nonzero Fermi level.[7,8] As discussed by Hwang and Sarma, although plasmons from both graphene and normal 2D electrons commonly show the $q^{1/2}$ dependence in the long wave length limit, the dispersions calculated within RPA including the finite wave-vector nonlocal effects appear to be quite different. Although the nonlocal correction for finite q causes a linearly decreasing $\omega(q)$ for graphene with increasing q, it produces increasing $\omega(q)$ for normal 2D systems.[7] Since our measured dispersion in Fig. 3 contains data with a wide range of q (0.024 Å$^{-1} \leqslant q \leqslant$ 0.144 Å^{-1}), we compare our dispersion with a calculated one using the full expression for polarizability including both $\Pi^+(q,\omega)$ and $\Pi^-(q,\omega)$ as described in Refs. 7 and 8.

As presented in Fig. 3, the measured dispersion of the intraband π plasmon from SLG is well described by this full polarizability (blue solid curve). For the calculated dispersion, we have fitted the data with an electron density n as the only fit parameter with reasonable values for other variables of a doped graphene, that is, a background dielectric constant $\kappa = (1 + \kappa_{SiC})/2 \approx 5.5$[7] and the Fermi velocity $v_F = 1.1 \times 10^6$ m/s.[2,4,19] We find $n = 1.2 \times 10^{13}$ cm^{-2} as the best fit value, which agrees well with those reported.[4,19] Furthermore, the Fermi energy and the Fermi wave vector obtained from n, $E_F = \hbar v_F k_F = 0.44$ eV and $k_F = \sqrt{n\pi} = 0.061$ Å^{-1}, agree quite well with previous estimations.[2,4,19] Here, we notice two distinct features of the intraband plasmon excitation from SLG: (1) It survives even in the interband SPE region for $q \geqslant q_c$, not significantly damped in intensity, and (2) its dispersion follows the linearly increasing boundary with q of the interband SPE region without ever penetrating into the intraband SPE. These peculiar features from SLG are completely different from the plasmon of a typical normal 2D electrons system.[15] One also notices that the plasmon from SLG decays, even for $q \leqslant q_c$, showing the increasing linewidth with q (see inset in Fig. 3). Such a damping may be caused by interacting with its own phonon of energy 200 meV as also seen in the Dirac band.[4,26]

In Fig. 3, we also compare our calculated dispersion (blue solid curve) with the Stern's full formula (light red curve), which entirely fails to reproduce our data even with the same values of electron density $n = 1.2 \times 10^{13}$ cm^{-2} and effective mass $m = 0.070\ m_e$.[14] Since plasmon is completely decayed for q beyond q_c due to the intraband SPE (Landau damping) for normal 2D electrons,[15,25] the Stern's formula is far from explaining the plasmon dispersion of SLG in Fig. 3. We also note that the dispersion of SLG in Fig. 3 having a $\omega \sim n^{1/4}$ dependence, especially for small q as predicted by theory, locates below the red curve having a $\omega \sim n^{1/2}$ dependence of a normal 2D system.[7]

As presented in Fig. 2(b), the loss peak L_3 upshifts in energy and splits into two peaks as FLG develops (see inset for fit details). The data points are for the two dispersions of intraband π plasmons from the two different FLGs in Fig. 4. The FLGs of $\hbar\omega_{FK} = 141$ meV and 149 meV are more than bilayer graphene, when compared with previous work.[12,13,23] Note that the dispersions tend to move away from the boundary between the inter- and intraband SPE regions with increasing q for $q \geqslant q_c$, unlike that of SLG. Such deviation in the plasmon dispersion for FLG may be produced by the presence of both optical as well as acoustical modes of excitations,[27] and also by the quasiparticles of finite mass from the parabolic π bands near the Dirac point.[2,27]

In summary, we have prepared a SLG-abundant sample formed on the insulating buffer phase in its early stage, and the dispersion of the low-energy intraband π plasmon measured from the sample appears to be quite distinct from that of normal 2D electrons or of FLG. The plasmon dispersion obtained from SLG with no multilayer effects is best described by a theoretical one derived for a doped SLG. We thus report another intrinsic feature of Dirac fermions in SLG stemming from its unique quantum relativistic character. We also identify several loss peaks characteristic to the intermediate phases during the graphitization process on SiC substrate, which may be used as a convenient *in situ* probe to sensitively identify the formation of SLG.

ACKNOWLEDGMENTS

This work was supported by the Korea Science and Engineering Foundation (KOSEF) funded by the Korea government (MEST) under Grant No. R01-2008-000-20020-0, and also in part by the NCRC under Grant No. R15-2008-006- 01001-0.

*jwc@postech.ac.kr

[1] A. K. Geim and K. S. Novoselov, Nat. Mater. **6**, 183 (2007).
[2] T. Ohta, A. Bostwick, J. L. McChesney, T. Seyller, K. Horn, and E. Rotenberg, Phys. Rev. Lett. **98**, 206802 (2007).
[3] R. Balog, B. Jørgensen, L. Nilsson, M. Andersen, E. Rienks, M. Bianchi, M. Fanetti, E. Lægsgaard, A. Baraldi, S. Lizzit, Z. Sljivancanin, F. Besenbacher, B. Hammer, T. G. Pedersen, P. Hofmann, and L. Hornekær, Nat. Mater. **9**, 315 (2010).
[4] A. Bostwick, T. Ohta, T. Seyller, K. Horn, and E. Rotenberg, Nature Phys. **3**, 36 (2007).
[5] A. C. Ferrari, J. C. Meyer, V. Scardaci, C. Casiraghi, M. Lazzeri, F. Mauri, S. Piscanec, D. Jiang, K. S. Novoselov, S. Roth, and A. K. Geim, Phys. Rev. Lett. **97**, 187401 (2006).
[6] Z. H. Ni, W. Chen, X. F. Fan, J. L. Kuo, T. Yu, A. T. S. Wee, and Z. X. Shen, Phys. Rev. B **77**, 115416 (2008), and references therein.
[7] E. H. Hwang and S. Das Sarma, Phys. Rev. B **75**, 205418 (2007).
[8] B. Wunsch, T. Stauber, F. Sols, and F. Guinea, New J. Phys. **8**, 318 (2006).
[9] J. Lu, K. P. Loh, H. Huang, W. Chen, and A. T. S. Wee, Phys. Rev. B **80**, 113410 (2009).
[10] C. Kramberger, R. Hambach, C. Giorgetti, M. H. Rummeli, M. Knupfer, J. Fink, B. Buchner, L. Reining, E. Einarsson, S. Maruyama, F. Sottile, K. Hannewald, V. Olevano, A. G. Marinopoulos, and T. Pichler, Phys. Rev. Lett. **100**, 196803 (2008).
[11] Y. Liu, R. F. Willis, K. V. Emtsev, and Th. Seyller, Phys. Rev. B **78**, 201403(R) (2008).
[12] Y. Liu and R. F. Willis, Phys. Rev. B **81**, 081406(R) (2010).
[13] T. Langer, J. Baringhaus, H. Pfnür, H. W. Schumacher, and C. Tegenkamp, New J. Phys. **12**, 033017 (2010).
[14] C. Tegenkamp, H. Pfnür, T. Langer, J. Baringhaus, and H. W. Schumacher, J. Phys. Condens. Matter **23**, 012001 (2011).
[15] F. Stern, Phys. Rev. Lett. **18**, 546 (1967).
[16] R. M. Tromp and J. B. Hannon, Phys. Rev. Lett. **102**, 106104 (2009).
[17] C. G. Hwang, S. Y. Shin, S. M. Choi, N. D. Kim, S. H. Uhm, H. S. Kim, C. C. Hwang, D. Y. Noh, S. H. Jhi, and J. W. Chung, Phys. Rev. B **79**, 115439 (2009).
[18] C. Riedl, A. A. Zakharov, and U. Starke, Appl. Phys. Lett. **93**, 033106 (2008).
[19] T. Seyller, A. Bostwick, K. V. Emtsev, K. Horn, L. Ley, J. L. McChesney, T. Ohta, J. D. Riley, E. Rotenberg, and F. Speck, Phys. Status Solidi B **245**, 1436 (2008).
[20] I. Forbeaux, J.-M. Themlin, and J.-M. Debever, Phys. Rev. B **58**, 16396 (1998).
[21] J. R. Ahn, S. S. Lee, N. D. Kim, C. G. Hwang, J. H. Min, and J. W. Chung, Surf. Sci. Lett. **516**, L529 (2002).
[22] C. Benesch, M. Fartmann, and H. Merz, Phys. Rev. B **64**, 205314 (2001).
[23] T. Angot, M. Portail, I. Forbeaux, and J. M. Layet, Surf. Sci. **502-503**, 81 (2002).
[24] P. Laitenberger and R. E. Palmer, Phys. Rev. Lett. **76**, 1952 (1996).
[25] T. Nagao, T. Hildebrandt, M. Henzler, and S. Hasegawa, Phys. Rev. Lett. **86**, 5747 (2001).
[26] M. Bianchi, E. D. L. Rienks, S. Lizzit, A. Baraldi, R. Balog, L. Hornekær, and P. Hofmann, Phys. Rev. B **81**, 041403(R) (2010).
[27] E. H. Hwang and S. Das Sarma, Phys. Rev. B **80**, 205405 (2009).